Available online at www.sciencedirect.com

ScienceDirect

Procedia Structural Integrity 2 (2016) 3057–3064

Structural Integrity Procedia

www.elsevier.com/locate/procedia

21st European Conference on Fracture, ECF21, 20-24 June 2016, Catania, Italy

Influence of the Casting Process in High Temperature Fatigue of A319 Aluminium Alloy Investigated By In-Situ X- Ray Tomography and Digital Volume Correlation

Nora Dahdah[a,*], Nathalie Limodin[a], Ahmed El Bartali[a], Jean-François Witz[a], Rian Seghir[a], Eric Charkaluk[a], Jean-Yves Buffiere[b]

[a] *Laboratoire de Mécanique de Lille (LML), FRE CNRS 3723; Ecole Centrale de Lille, 59651 Villeneuve d'Ascq cedex, France*
[b]*Laboratoire Matériaux, Ingénierie et Sciences (MATEIS), INSA-Lyon, CNRS UMR 5510; Villeurbanne, 69621, France*

Abstract

In order to satisfy the economic constraints together with environmental requirements, the automotive industry has been forced to adopt a strategy of down-sizing, which has led into process modification of some engine parts like cylinder heads. Nowadays, the Lost Foam Casting process (LFC) replaces the conventional Die Casting (DC) process due to cost reduction and geometry optimization goals. However, aluminum alloy automotive parts produced by the LFC process have a coarser microstructure and more porosity defects than parts produced with conventional casting processes at faster cooling rates. In the cylinder heads produced by the LFC process, the microstructure consists of hard intermetallic phases and large gas and microshrinkage pores. In order to study the influence of this complex 3D microstructure on fatigue crack initiation and propagation, an experimental protocol using laboratory, synchrotron tomography, SEM images and 3D Digital Volume Correlation (DVC) has been used. Fatigue tests performed at temperatures characteristics of in-service conditions (250°C) revealed the initiation of 3D cracks at large pores and a propagation along the hard inclusions around the main pore that drove to failure but also in other areas of the specimen gauge length.

Peer-review under responsibility of the Scientific Committee of ECF21.

Keywords: Aluminum-silicon alloys, High Temperature, Digital Volume Correlation, synchrotron X-ray tomography

* Corresponding author. Tel.: +33-(0)6-95-24-66-25; fax: +33-(0)3-20-33-53-93
E-mail address: nora.dahdah@ec-lille.fr

Copyright © 2016 The Authors. Published by Elsevier B.V. This is an open access article under the CC BY-NC-ND license (http://creativecommons.org/licenses/by-nc-nd/4.0/).
Peer review under responsibility of the Scientific Committee of ECF21.
10.1016/j.prostr.2016.06.382

1. Introduction

The performance of an automotive engine is provided for a large part by the cylinder head. During the start-stop of the vehicle, the cylinder head is subjected to high thermal variations between 20°C and 250°C. The parts near the combustion chamber are subjected to Low Cycle Fatigue (LCF). In order to satisfy the economic constraints together with environmental requirements, the automotive industry has been forced to adopt a strategy of "down-sizing" that has led into process modification of some engine parts like cylinder heads. Nowadays, the Lost Foam Casting process (LFC) replaces the conventional Die Casting (DC) process for the purpose of geometry optimization, cost reduction and consumption control. LFC uses almost a quarter less energy and a third less molten metal than conventional casting (Shivkumar et al., 1990). The advantages of LFC over DC process are above all the low cost of foam, unbounded sand, possibility of complex shapes with internal channels and finishing costs (Albonetti, 2000). The main disadvantage of LFC is the presence of defects which are caused by entrapment of gases in the solidifying metal. Moreover, LFC process cooling rate is relatively slow compared with DC process (LFC around $0.8°C.s^{-1}$ and DC around 30°C.s−1)(Albonetti, 2000). This leads to a coarser microstructure when measured in term of Dendrite Arm Spacing (DAS). Besides, the porosity and inclusions (eutectic Si, eutectic Al–Al_2Cu, and iron based intermetallics) are increased and clustered. The microstructure of the A319 produced by the LFC process is a complex network of very large particles: Silicon particles, Al_2Cu, α-AlFeSi, β-AlFeSi and pores. Pores (Wang, Q.G et al., 2001) can play a decisive role above a critical size, by providing preferential crack initiation sites but an influence of the other phases such as oxides (Cao et al., 2003), iron-based intermetallics (Tabibian et al., 2013) and Si particles (Buffière et al., 2001) is also observed.

The present work focuses on the use of an experimental protocol using synchrotron tomography, SEM observations and 3D digital volume correlation to study the influence of the casting microstructure at high temperature upon the fatigue behavior. The mechanisms of initiation and propagation in the A319 alloy will be studied in details. The main objective of the experiment is to obtain in situ 3D images of the initiation and growth of damage during cyclic mechanical loading of an Aluminum Silicon automotive cast alloy (A319) at temperatures relevant for service conditions (T=250°C).

2. Experimental procedure

The material studied was an A319 aluminum silicon alloy (Al bal.– Si 7.18 wt.% – Mg 0.32 wt.% – Mn 0.15 wt.% – Cu 3.17 wt.% –Fe 0.43 wt.% – Ti 0.05 wt.%). Small dog-bone specimens with a $2.6x2.6mm^2$ cross section were spark cut from the most severely stressed area of A319 cylinder heads. The first stage of the experimental protocol is to select the most suitable specimens, i.e the specimens having no large defects close to the shoulders(Wang, 2015). This step allows focusing the X-ray tomography observation during the fatigue test on a volume where cracks are likely to initiate. A preliminary step using laboratory X-ray tomography was thus performed at the LML laboratory in fast scan mode with a 80 kV acceleration voltage to ensure a 10% transmission of the X-ray beam through the cross-section of the sample. The scan was made at a medium resolution with a voxel size of 4.5µm; this medium resolution images allow revealing the size and shape of the large pores in the bulk of the specimens gauge length rapidly. Two fatigue specimens are selected, then mechanically polished on all faces down to a 2x2 mm^2 cross section using SiC paper of grades up to 4000 grits and diamond suspension up to 1/4 µm. In-situ fatigue tests at 250°C were performed on ID19 at the European Synchrotron Radiation Facility (ESRF). In this paper, only one specimen is studied.

A radiation furnace designed by the Centre des Matériaux (Ecole des Mines de Paris) is equipped with four halogen lamps (Dezecot et al., 2016) (Fig.1.a) and is used with a fatigue machine developed at MATEIS laboratory (Fig.1.b). A quartz tube allows transmitting the load from the top to the bottom of the machine. Images were obtained in pink beam mode (E=35 keV) on a CMOS PCO Dimax detector (2048 $pixels^2$). The scan duration was 45 s (2000 Images) with a 2.75 µm voxel size. Thanks to the large spatial coherence of the beam on ID19 phase contrast could be obtained, so that eutectic Si particles could be easily distinguished from the surrounding Al matrix and small cracks could easily be detected. The scan time was short enough to avoid creep/relaxation effects at the temperatures

investigated. Uniaxial tensile fatigue tests at constant stress amplitude were performed with a load ratio of 0.1 and a maximum stress of the order of 150% of the yield stress at the corresponding temperature.

Synchrotron tomography allowed to visualize the eutectic Al–Al_2Cu, iron based intermetallics phases and above all eutectic Si, which could not be distinguished with laboratory tomography; these constituents were proved a suitable natural speckle for Digital Volume Correlation. The 3D strain field was measured with the DVC technique (Rethore et al., 2011), which is an extension of the well-developed Digital Image Correlation (DIC) method. In the present study, a 3D image correlation platform called YaDICs (Seghir et al., 2015) newly developed at LML laboratory has been used. The DVC measurement (Dahdah et al., 2016) was performed between the reference image at minimum load and the deformed image at maximum load of each considered cycle. The fracture surfaces after tensile test were examined with a JEOL 7800 F LV SEM, coupled with energy-dispersive X-ray spectroscopy (EDX).

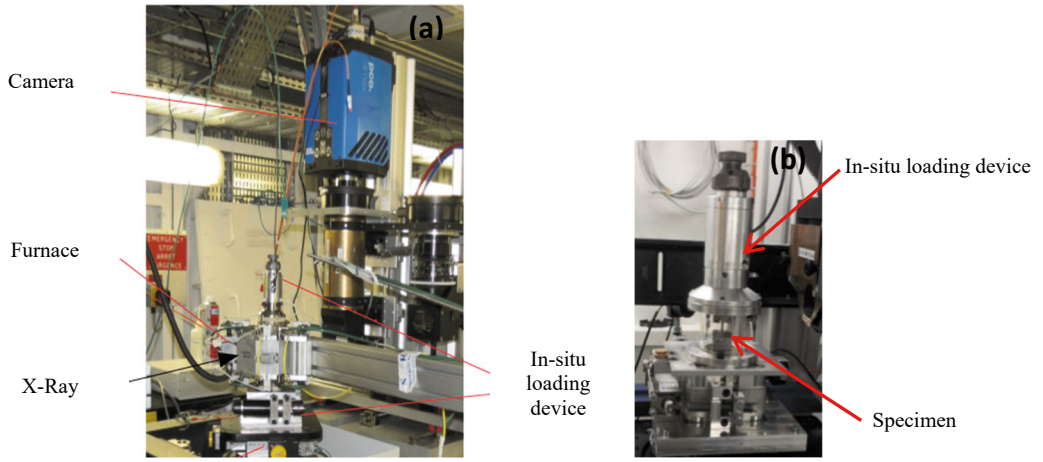

Fig.1. In situ fatigue test with: (a) Experimental set-up with a close-up view on the (b) Fatigue machine

3. Results and discussion

3.1 Microstructure analysis

The test on the specimen studied was realized at a maximum stress of 75MPa. The synchrotron scans were performed at the minimum and maximum stress of the fatigue cycle until the failure occurred at 50 cycles. An observation of all the slices at different numbers of cycles was made in order to link the crack initiation to a specific cycle. Thus, only a limited number of cycles were studied for the DVC measurements: the 1st cycle of the fatigue test, which consists in the reference image, i.e. the image of the minimum load before any cycle loading, and also the image

at the maximum load where the crack initiation appeared, the 10th cycle where the crack propagation started, and the 30th cycle to follow the crack propagation.

The analyzed specimen, as well as all the others selected samples contains a high number of pores in the gauge length volume (Fig.2.a). The volume fraction of pores is about 0.8%. The distribution of Feret diameter of these pores shows a peak around 15µm with a maximum Feret diameter of 1200µm. Although scarce in number, the largest pores represent most of the pores volume fraction.

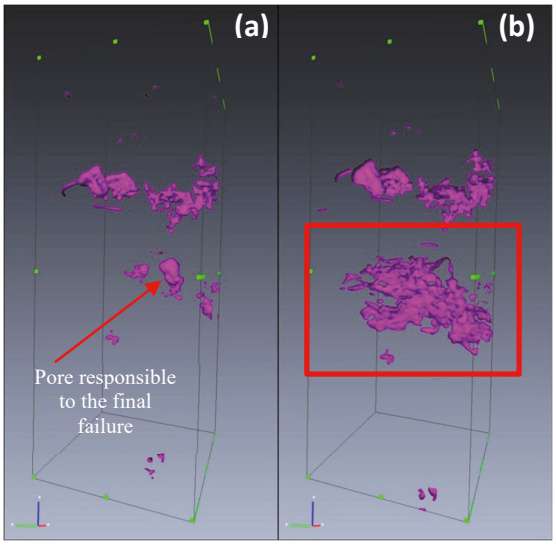

Fig.2. (a) 3D Rendering of pores in the fatigue test specimen before the fatigue test, (b) at the 40th cycle before failure with the red square representing the final failure zone

The microstructure of A319 alloy is presented in Fig.3 in order to distinguish easily the shapes of the different constituents of the microstructure: pores, Al_2Cu phase, eutectic Si-particles and iron-based intermetallic phases. A quantitative analysis highlights a volume fraction of hard inclusions about 17% including about 9% of eutectic Si, 7% of iron-based intermetallics and 1% of Al_2Cu phases (Wang, 2015). In Fig.3, the 2 types of iron intermetallic phases can be distinguished, the α(AlFeMnSi) phase with a structure known as "Chinese script" and β(AlFeSi) phase in platelets shape. Silicon phase has a plate like morphology. Al_2Cu phases is also observed, it forms a block between the eutectic Si phase and the intermetallics phases.

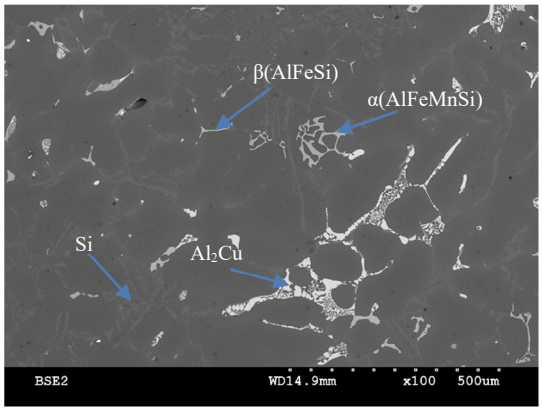

Fig.3 SEM image of A319 alloy showing the complex microstructure

3.2 Initiation and propagation mechanisms

The Fig.4 showing the microstructure of the A319 alloy before the fatigue test (Fig.4.a) and after the first tensile loading (Fig.4.b) allows the observation of crack initiation close to a large pore. For all the specimens studied, the crack initiated always close to a large pore during the first tensile loading. However, the propagation (Fig.5.b&c) appears along the hard inclusions including silicon phase, iron intermetallics and copper containing phases. This propagation phenomena is similar to micro-cracks above all observed in the silicon phase (see red circle in Fig.5.c). The crack localization appears between different pores, due to high stress concentrations induced by the large size of pores inherited from the LFC process but also because of the location of the pore that is notably close to the surface. Then, the crack propagation is affected by the coalescence of the micro-cracks between the pores especially the micro-cracks in the silicon phase.

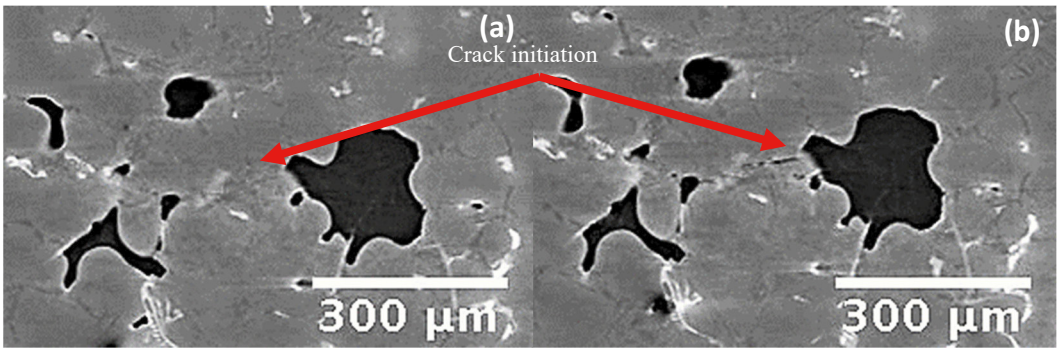

Fig.4. Microstructural observation at the first cycle: (a) minimum loading, (b) maximum loading

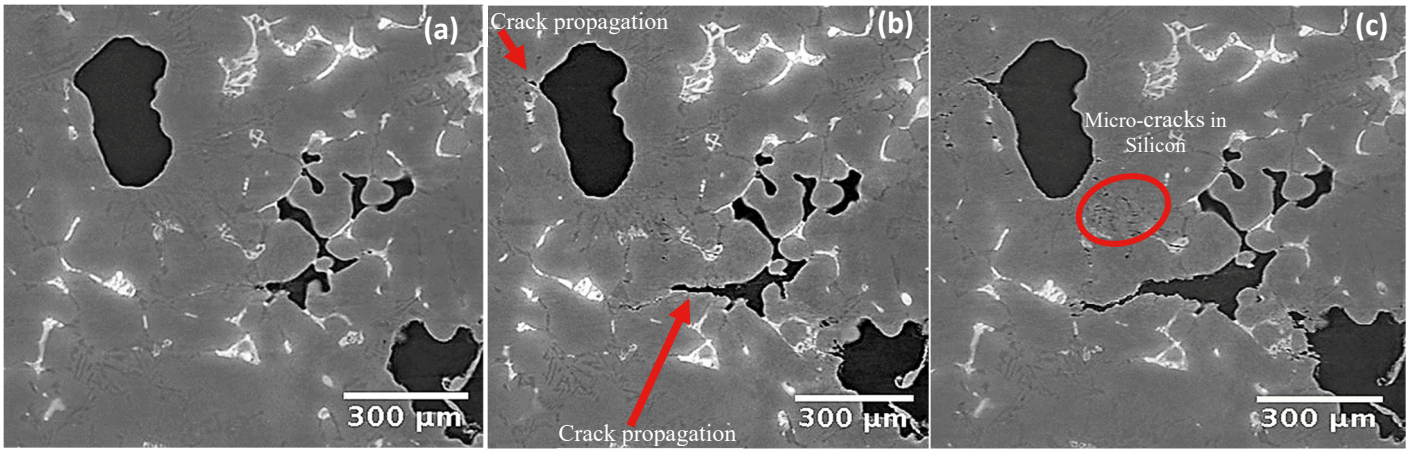

Fig.5. Observation of the microstructure at (a) 0c, (b) 10c, (c) 30c a the maximum loading

3.3 Postmortem analysis

SEM observations were performed on the specimens after the failure. Fig. 6 shows the final crack on the sample tested at 250°C. Post-mortem observations confirmed the analyses done before. Indeed, on the failure zone (Fig.6.a)

several phases seem to be broken, particularly the silicon phase and this phenomenon occurred also in the zone far away from the principal crack (Fig.6.b). The cracking of silicon is observed in whole volume of the specimen. To understand the major role of the Si particles for the propagation of damage, there are some explanations as they form an extended network (Asghar et al., 2011)(Lasagni et al., 2008) in the entire volume of the specimen, but also Si particles have a coarser morphology which create large stress concentration (Barrirero et al., 2013) and the eutectic silicon is more brittle than other hard inclusions at high temperature (Chen et al., 2006). Besides, according to Joyce (Joyce et al., 2003), the thermal expansion coefficient difference between Si and Al indicates that thermal cycling is likely to lead to cracking or decohesion of larger Si particles due to significant strain mismatch.

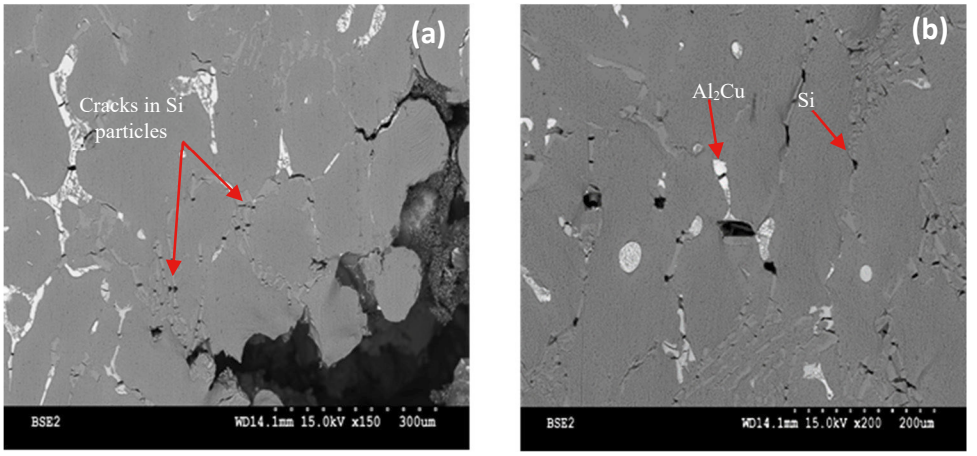

Fig.6. (a) SEM image in the zone around the final fracture, (b) in a zone faraway to the final fracture

X-ray mappings were performed on the fracture surfaces of fatigue specimens to identify the damage mechanisms of hard inclusions. X-ray mappings were only performed on the area where the crack was observed to propagate during the in-situ fatigue (Fig.7.a). Both fracture surfaces images of the specimen are placed side by side (Fig.7.b). If the same constituents are identified in the same location on both fracture surfaces, the failure mechanism is fracture of hard particles. Otherwise, the failure mechanism is decohesion/debonding. For the silicon phase, quite the same proportion of decohesion (see the red arrows in Fig.7.b) and fracture (see the yellow arrows in Fig7.a) is found in cracks propagations regions. However, during the in-situ fatigue test the failure mechanism seems to be more multi fracture in the hard phases than decohesion.

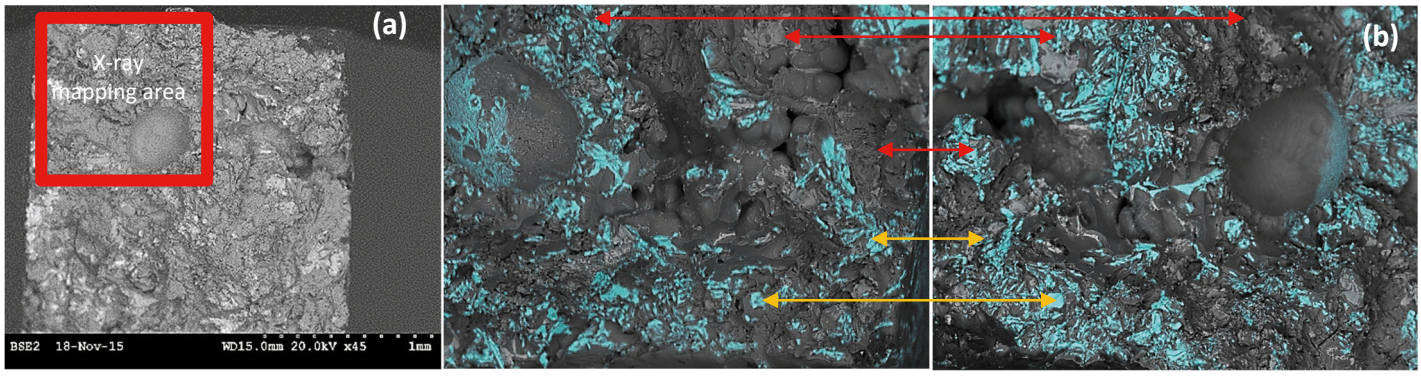

Fig.7. (a) SEM images illustrating X-ray mapping area location, (b) X-ray mapping images of two

fracture surfaces of the same specimen showing in red the decohesion mechanism and in yellow the fracture mechanism

3.4 DVC measurement

The strain fields were computed by DVC in the zone of the sample containing the pore which has led to progressive crack growth until final failure (red square shown in Fig.2.b) and it is shown with the arrow in Fig. 2.a. Fig. 8 shows the strain field along the loading direction; the image of the microstructure was superposed to these fields to allow comparison of the crack path with local deformation. The fields were studied at different steps of the fatigue cycles. The Fig. 8 show strain fields at the first cycle (Fig.8.a), at the 10th cycle (Fig.8.b) and at the 30th cycle (Fig.8.c). At the first cycle (Fig.8.a), a strain localization is well observed in the area where the nucleation of the crack is visible. Then after 10 cycles, a strain localization is localized where the propagation of the crack is observed and after 30 cycles, the strain localization increased where crack growth is the most important. The Fig.8.d allows a better visualization of the microstructure in the crack neighborhood, the pores are represented in blue and the microstructure shows the crack growth at the 50th cycles of loading, just before the failure. A good correlation is observed between the crack location and the strain localizations. The DVC analysis of the 3D images recorded in situ helps to understand the relations between initiation sites and crack path and the local microstructural features: crack initiation is porosity driven while propagation is correlated with the presence of hard intermetallic phases and silicon phase.

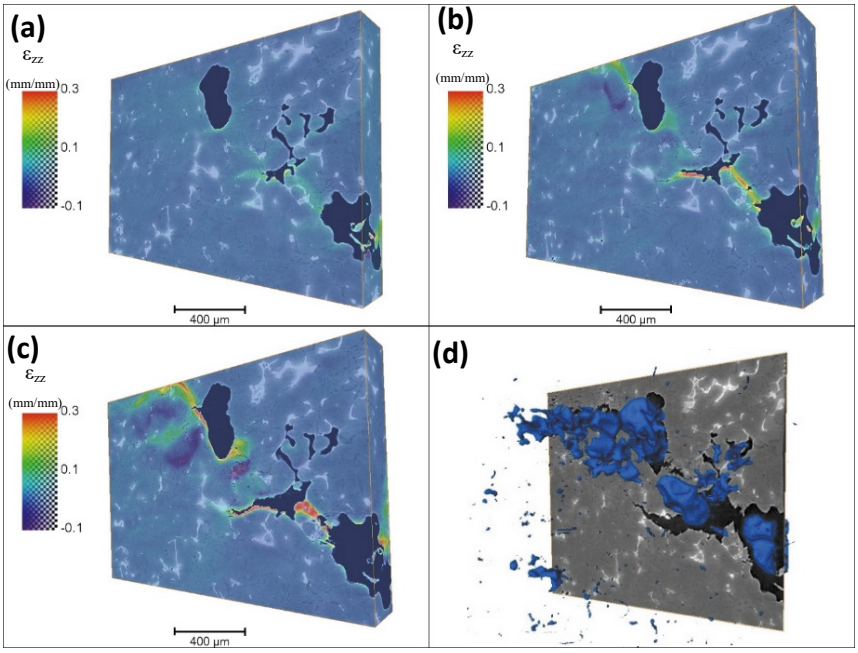

Fig.8 ε_{zz} strain field with the microstructure shown in transparency (a) at 1c, (b) 10c, (c) 30c and (d) the fracture surface at 40c before failure

4. Conclusions

The efficiency of the experimental protocol using laboratory and synchrotron tomography, SEM images and 3D digital volume correlation to study the influence of the casting microstructure upon the mechanical properties at high temperature of an Al-Si alloy has been proved. The 3D images obtained by synchrotron tomography allow the characterization of the complex microstructure in the A319 alloy. The DVC analysis helps to understand the relations between initiation sites and crack path and the local microstructural features: crack initiation is porosity driven while propagation is correlated with the presence of hard intermetallic phases, and above all the micro-cracks in the silicon particles. The method illustrated here will now be systematically used to analyze the fatigue behavior of the other samples tested during the ESRF fatigue experiment in order to make correlations between initiation sites and crack path and the local microstructural features.

Acknowledgements

The authors wish to thank the ANR (Agence Nationale de la Recherche) MatetPro project INDiANA for funding the study on Al-Si aluminum alloys. The ESRF (European Synchrotron Radiation Facility) is also acknowledged for providing beamtime on the ID19 beamline; Elodie Boller and Vincent Fernandez from ESRF are particularly acknowledged for their help and advices with the Synchrotron tomography experiment. The ISIS4D X-Ray CT platform has been funded by International Campus on Safety and Intermodality in Transportation (CISIT), the Nord-Pas-de-Calais Region, the European Community and the National Center for Scientific Research. The authors gratefully acknowledge the support of these institutions.

References

Albonetti, R., 2000. Porosity and Intermetallic Formation in Lost Foam Casting of 356 Alloy. The University of Western Ontario London. Thesis

Asghar, Z, Requena, G., Boller, E., 2011. Three-dimensional rigid multiphase networks providing high-temperature strength to cast AlSi10Cu5Ni1-2 piston alloys. Acta materialia, 59(16), 6420–6432.

Barrirero, J., Engstler, M., Mücklich, F., 2013. Atom Probe Analysis of Sr Distribution in AlSi Foundry Alloys. In In Light Metals 2013, B.A. Sadler, ed. (John Wiley & Sons, Inc.), 289–296.

Cao, X., Campbell, J., 2003. The nucleation of Fe-rich phases on oxide films in Al-11.5 Si-0.4 Mg cast alloys. Metallurgical and Materials Transactions A, 34(July), 1409–1420.

Chen, C.L., West, G.D., Thomson, R.C., 2006. Characterisation of Intermetallic Phases in Multicomponent Al-Si Casting Alloys for Engineering Applications.

Dahdah, N, Limodin, N, El Bartali, A, Witz, J-F, Charkaluk, E, Buffière, J-Y, 2016. Damage investigation in a319 aluminium alloy by x- ray tomography and digital volume correlation during in situ high temperature fatigue tests. Strain, (Submitted).

Dezecot, S, Buffière, J-Y, Koster, A, Maurel, V, Szmytka, F, Charkaluk, E, Dahdah, N, El Bartali, A, Limodin, N, Witz, J-F, 2016. In situ 3D characterization of high temperature fatigue damage mechanisms in a cast aluminum alloy using synchrotron X-ray tomography. Scripta Materialia 113, 254–258.

Joyce, M.R., Styles, C.M. and Reed, P.A.S., 2003. Elevated temperature short crack fatigue behaviour in near eutectic Al-Si alloys. International Journal of Fatigue. 863–869.

Lasagni, F, Lasagni, A, Engstler, M, Degischer, H.P, Mucklich, F, 2008. Nano-characterization of Cast Structures by FIB-Tomography. Advanced Engineering Materials, 10(1-2), 62–66.

Réthoré, J, Limodin, N, Buffière, J-Y, Hild, F, Ludwig, W, Roux, S, 2011. Digital volume correlation analyses of synchrotron tomographic images. The Journal of Strain Analysis for Engineering Design, 46(7), 683–695.

Shivkumar,S,Wang,L, Apelian, D, 1990. The lost-foam casting of aluminium alloy components,

Buffière, J.-Y., Savelli, S., Jouneau, P.H., Maire, E., Fougères, R, 2001. Experimental study of porosity and its relation to fatigue mechanisms of model Al–Si7–Mg0.3 cast Al alloys. , Materials science & engineering A316, 115–126.

Seghir, R., Witz, J.F., Coudert, S., YaDICs - Digital Image Correlation 2/3D software. http://www.yadics.univ-lille1.fr/wordpress,.

Tabibian, S., Charkaluk, E., Constantinescu, A., Szmytka, F., Oudin, A. 2013. TMF–LCF life assessment of a Lost Foam Casting A319 aluminum alloy. International Journal of Fatigue, 53, 75–81.

Wang, L, 2015. Influence of the casting microstructure on damage mechanisms in Al-Si alloys by using 2D and 3D in-situ analysis.Thesis

Wang, Q.G., Apelian, D., Lados, D.A., 2001. Fatigue behavior of A356/357 aluminum cast alloys. Part II ± Effect of microstructural constituents., Light Met. 1, 85–97